Pergamon

0043-1354(95)00056-9

Wat. Res. Vol. 29, No. 10, pp. 2247–2254, 1995

0043-1354/95 $9.50 + 0.00

AIR–WATER GAS TRANSFER AT HYDRAULIC JUMP WITH PARTIALLY DEVELOPED INFLOW

HUBERT CHANSON

Department of Civil Engineering, The University of Queensland, Brisbane, Qld 4072, Australia

(First received October 1994; accepted in revised form February 1995)

Abstract—In open channels, the transition from a rapid to fluvial flow is called a hydraulic jump. It is characterized by large scale turbulence, air bubble entrainment and energy dissipation. The author has investigated the air bubble entrainment at hydraulic jumps with partially developed inflow conditions. The air–water flow is characterized by a turbulent shear region with a large air content which contributes to the enhancement of the air–water interface area and air–water gas transfer in the hydraulic jump. A new gas transfer model is presented. Based upon physical evidence, the model enables prediction of the dissolved gas contents and water quality downstream of hydraulic jumps with partially developed inflows.

Key words—air–water gas transfer, air entrainment, hydraulic jump, partially developed inflow

NOMENCLATURE

a = specific interface area (m^{-1}): air–water surface area per unit volume of air and water
C = air concentration: volume of air per unit volume of air and water
C_{DS} = downstream dissolved gas concentration (kg/m^3)
C_{US} = upstream dissolved gas concentration (kg/m^3)
C_{gas} = concentration of dissolved gas in water (kg/m^3)
C_{max} = maximum air concentration in the turbulent shear region of a hydraulic jump
$(C_{max})_1$ = maximum air concentration in the turbulent shear region at the jump toe
C_s = gas saturation concentration in water (kg/m^3)
d = flow depth (m) measured perpendicular to the channel bottom
d_{ab} = air bubble diameter (m)
$(d_{ab})_{max}$ = maximum bubble size (m) in the shear flow region of a hydraulic jump
$(d_{ab})_{mean}$ = mean bubble size (m) in the shear flow region of a hydraulic jump
d_c = critical flow depth (m): for a rectangular channel: $d_c = \sqrt[3]{q_w^2/g}$
E = aeration efficiency defined as: $E = 1-1/r$
Fr = Froude number defined as: $Fr = q_w/\sqrt{g*d^3}$
Fr_e = Froude number at the inception of air entrainment: $Fr_e = V_e/\sqrt{g*d}$
g = gravity constant: $g = 9.80$ m/s^2 in Brisbane, Australia
K_L = liquid film coefficient (m/s)
K', k' = constant of proportionality
L_a = aeration length (m) of the hydraulic jump
L_r = roller length (m)
Q_{air}^{HJ} = quantity of air entrained (m^3/s) by hydraulic jump
Q_w = water discharge (m^3/s)
q_w = water discharge per unit width (m^2/s)
Re = Reynolds number: $Re = q_w/\nu_w$
r = deficit ratio: $(C_s - C_{US})/(C_s - C_{DS})$
T = temperature (K)
t_1 = time (s)
t_2 = residence time (s) of air bubbles in a hydraulic jump
V = velocity (m/s)
V_e = onset velocity (m/s) for air entrainment
V_1 = upstream flow velocity (m/s): $V_1 = q_w/d_1$
W = channel width (m)
x = distance along the channel bottom (m) measured from the sluice gate
x_1 = location (m) of the jump toe measured from the sluice gate
y = distance (m) measured perpendicular to the channel surface
y_{Cmax} = distance measured perpendicular to the channel bottom where $C = C_{max}$
α_1, α_2, α_3 = constants
ΔH = head loss (m)
$\Delta Y_{85\%}$ = 85%-band width (m): i.e. where $C = 0.85*C_{max}$
δ_{99} = boundary layer thickness (m) defined in terms of 99% of the free-stream velocity
ν_w = kinematic viscosity (m^2/s)

subscript
1 = flow conditions upstream of the hydraulic jump
2 = flow conditions downstream of the hydraulic jump
15,20 = flow properties at 15, 20, 25°C

INTRODUCTION

In open channel flow, the transition from a rapid (supercritical) to a tranquil (subcritical) flow is called a hydraulic jump. It is characterized by the development of large-scale turbulence, surface waves and spray, energy dissipation and air entrainment. The large-scale turbulence region is usually called the "roller". The roller length can be estimated as (Hager *et al.*, 1990):

$$\frac{L_r}{d_1} = 8*(Fr_1 - 1.5) \qquad (1)$$

where d_1 is the upstream flow depth and Fr_1 is the upstream Froude number.

For a prismatic horizontal channel, the flow conditions downstream of a hydraulic jump are

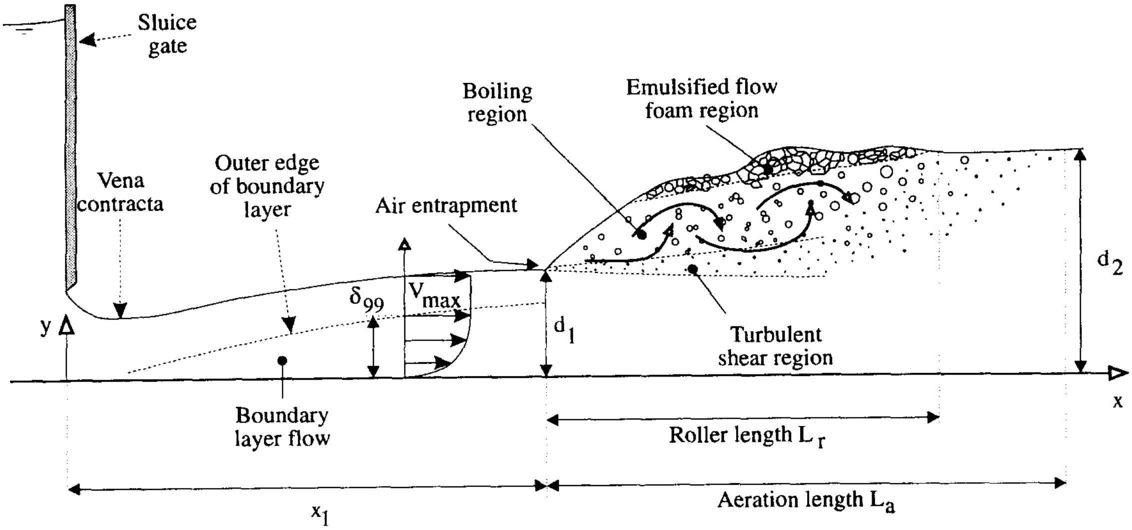

Fig. 1. Air–water flow region of a hydraulic jump.

functions typically of the discharge, upstream depth and channel shape (e.g. Henderson, 1966). However, the jump characteristics are also functions of the inflow conditions. In a horizontal rectangular channel, three types of inflow conditions are distinguished: a partially developed supercritical flow, a fully developed boundary layer flow and a pre-entrained jump. A partially developed jump exhibits a developing boundary layer and a quasi-potential flow core above (Fig. 1). For a fully-developed jump, the boundary layer has expanded over the entire flow depth. A pre-entrained jump is a fully-developed jump with free-surface aeration. The air–water mixture next to the free-surface modifies the jet impingement and hence the roller characteristics.

With any inflow configuration, large quantities of air are entrained at the toe of a jump. Air bubbles are entrapped by vortices with axes perpendicular to the flow direction. The entrained bubbles are advected downstream into a free shear layer characterized by intensive turbulence production before reaching the free-surface and escaping to the atmosphere. A re-analysis of the data of Rajaratnam (1962, 1967) showed that the aeration length can be estimated as (Hager, 1992):

$$\frac{L_a}{d_2} = 3.5^*\sqrt{\mathrm{Fr}_1 - 1.5} \tag{2}$$

where d_2 is the downstream flow depth (Fig. 1).

Several studies (Table 1) showed that the quantity of air entrained can be estimated as:

$$Q_{\mathrm{air}}^{\mathrm{HJ}} = K'^*(V_1 - V_e)^n \tag{3}$$

where V_1 is the inflow velocity and V_e is the velocity at which air entrainment commences. Experimental results with hydraulic jumps (Table 1) and at vertical plunging jets (Ervine *et al.*, 1980) suggest that the inception velocity V_e is almost constant for turbulent flows with typical values of about 0.8-1 m/s. In engineering practice, equation (3) is estimated using the correlations of Rajaratnam (1967) and Wisner (1965).

Air entrainment at hydraulic jumps has been recognized recently for its contribution to the

Table 1. Inception velocity of air entrainment and quantity of entrained air by hydraulic jumps

Reference (1)	Geometry (2)	V_e (m/s) (3)	$Q_{\mathrm{air}}^{\mathrm{HJ}}/Q_w$ (4)	Comments (5)
Kalinske and Robertson (1943)	Hydraulic jump in a horizontal circular pipe	1.0	$0.0066^*(\mathrm{Fr}_1-1)^{1.4}$	Model data. $2 < \mathrm{Fr}_1 < 25$
Wisner (1965)	Hydraulic jump in a rectangular conduit	$\mathrm{Fr}_e = 1$	$0.014^*(\mathrm{Fr}_1-1)^{1.4}$	Prototype data. $5 < \mathrm{Fr}_1 < 25$
Rajaratnam (1967)	Hydraulic jump in a rectangular channel		$0.018^*(\mathrm{Fr}_1-1)^{1.245}$	Model data. $2.4 < \mathrm{Fr}_1 < 8.7$
Casteleyn *et al.* (1977)	Siphon of square cross-section	0.8	$q_{\mathrm{air}}^{\mathrm{HJ}} = k^*(V_1-V_e)^3$	Model data ($W = 0.43$ and 0.15 m). $1 < V_1 < 2.8$ m/s
Ervine and Ahmed (1982)	Two-dimensional vertical dropshaft	0.8	$q_{\mathrm{air}}^{\mathrm{HJ}} = 0.00045^*(V_1-V_e)^3$	Model data. Vertical jets. $3 < V_1 < 6$ m/s
Rabben *et al.* (1983)	Hydraulic jump in horizontal pipes	$\mathrm{Fr}_e = 1$	$0.03^*(\mathrm{Fr}_1-1)^{0.76}$	Model data. Gate opening: 1/4
Chanson (1993)	Hydraulic jump in a rectangular channel	0.66–1.41		$W = 0.25$ m. Fully developed upstream shear flow

Fr_e = Froude number defined in terms of the inception velocity: $\mathrm{Fr}_e = V_e/\sqrt{g^*d_1}$

Table 2. Oxygen transfer correlations at hydraulic jumps

Reference (1)	Formula (2)	Remarks (4)
Holler (1971)	r_{20}-1 = 0.0463*ΔV^2	Model experiments: $0.61 < \Delta V < 2.44$ m/s 277.15«it > T < 299.15 K
Apted and Novak (1973)	$r_{15} = 10^{(0.24*\Delta H)}$	Model experiments: $2 < Fr_1 < 8$ $q_w = 0.04$ m^2/s
Avery and Novak (1975)	r_{15}-1 = 0.23*(q_w/0.0345)$^{3.4}$*($\Delta H/d1$)$^{4.5}$	Model experiments: $2 < Fr_1 < 9$ $1.45 \times 10^4 < Re < 7.1 \times 10^4$ 0.013«it > d_1 < 0.03 m 287.15«it > T < 291.15 K $W = 0.10$ m
Avery and Novak (1978)	r_{15}-1 = k'*$Fr_1^{2.1}$*$Re^{0.75}$ $k' = 1.0043 \times 10^{-6}$: tap water with 0% $NaNO_2$ $k' = 1.2445 \times 10^{-6}$: tap water with 0.3% $NaNO_2$ $k' = 1.5502 \times 10^{-6}$: tap water with 0.6% $NaNO_2$	Model experiments: $1.45 \times 10^4 < Re < 7.1 \times 10^4$ $\nu_w = 1.143 \times 10^{-6}$ m^2/s $W = 0.10$ m
Wilhelms *et al.* (1981)	r_{15}-1 = 4.924×10^{-8}*$Fr_1^{2.106}$*$Re^{1.034}$	Model experiments ($W = 0.381$ m) based on krypton-85 transfer: $1.89 < Fr_1 < 9.5$ $2.4 \times 10^4 < Re < 4.3 \times 10^4$
Johnson (1984)	Empirical fit based on field data from 24 hydraulic structures	Prototype data. Working well for deep plunge pools

ΔV = difference between the upstream and downstream velocities (m/s).
r_{15}, r_{20} = oxygen deficit ratio at 15 and 20°C.

air–water transfer of atmospheric gases such as oxygen and nitrogen. At a jump, both the flow aeration and the strong turbulent mixing enhance the gas transfer. Several researchers proposed empirical correlations to predict the oxygen transfer (Table 2), but none of the studies took into account the air–water flow characteristics nor the effects of turbulence.

In this paper, new experimental data are presented. The results provide new information on the air distribution in hydraulic jumps with partially developed inflow conditions. Then the author proposes a new gas transfer calculation method. The model is based upon experimental observations which provide new understanding on the air–water gas transfer process. The results are compared with gas transfer data.

EXPERIMENTAL APPARATUS

New experiments were performed in a 3.20-m long horizontal glass channel (0.25-m width). Waters were supplied from a head tank which feeds the channel through a vertical sluice gate (opening: 20 mm) and the observed flow depth immediately downstream of the gate was 12 mm. Such a contraction ratio is very close to the Von Mises' solution for the no-gravity case (e.g. Henderson, 1966) and to computational calculations (e.g. Isaacs and Allen, 1994). Tailwater levels were controlled by an overflow gate at the downstream end of the channel. Further details were provided by Chanson and Qiao (1994).

The flow depths were measured using a rail mounted pointer gauge positioned over the centreline of the channel ($\Delta d < 0.5$ mm). The upstream flow conditions (velocity and pressure distributions) were recorded using a Pitot tube. Air concentration measurements were performed with a single-tip conductivity probe similar as the design developed by Chanson (1988). The conductivity probe consists of a sharpened rod (platinum wire $\phi = 0.35$ mm) which is insulated except for its tip and set into a metal supporting tube (stainless steel surgical needle $\phi = 1.42$ mm) acting as the second electrode. The conductivity probe was excited by an air bubble detector (AS25240) connected to a digital multimeter. The electronic circuit, designed with a response time of less than 10 μs, was calibrated with a square wave generator.

The vertical translation of the Pitot tube and conductivity probe was controlled by a fine adjustment travelling mechanism connected to a Mitutoyo™ digimatic scale unit (Ref. No. 572-503) ($\Delta y < 0.1$ mm). The longitudinal translation of the probes was controlled manually ($\Delta x < 5$ mm).

Preparation of the experimental flow conditions

During the experiments, the toe of the jump was located between 0.45 and 1.1 m from the sluice gate. For such flow conditions, the upstream Froude numbers Fr_1 ranged from 5.02 up to 8.11. The upstream flows were partially developed boundary layers or near the transition between developing and developed shear flows (i.e. $0.45 < \delta_{99}/d_1 < 1$) (Chanson and Qiao, 1994). Visual records of the roller and aeration lengths closely matched equations (1) and (2), respectively.

EXPERIMENTAL RESULTS

Structure of the bubbly flow

Visual observations enabled a comprehensive description of the bubbly flow region of the hydraulic jump. The following summarizes the findings of the present study and the earlier investigations by Thandaveswara (1974), Resch and Leutheusser (1972), Resch *et al.* (1974) and Babb and Aus (1981).

The air–water flow region of the hydraulic jump can be divided into three sub-regions: (1) a turbulent shear layer with smaller air bubble sizes, (2) a "boiling" flow region characterized by the development of large-scale eddies and bubble coalescence and (3) a foam layer at the free-surface with large air polyhedra structures (Fig. 1).

Air entrainment occurs in the form of air bubbles and air pockets entrapped at the impingement of the upstream jet flow with the roller. The air pockets are broken up into very thin air bubbles as they are

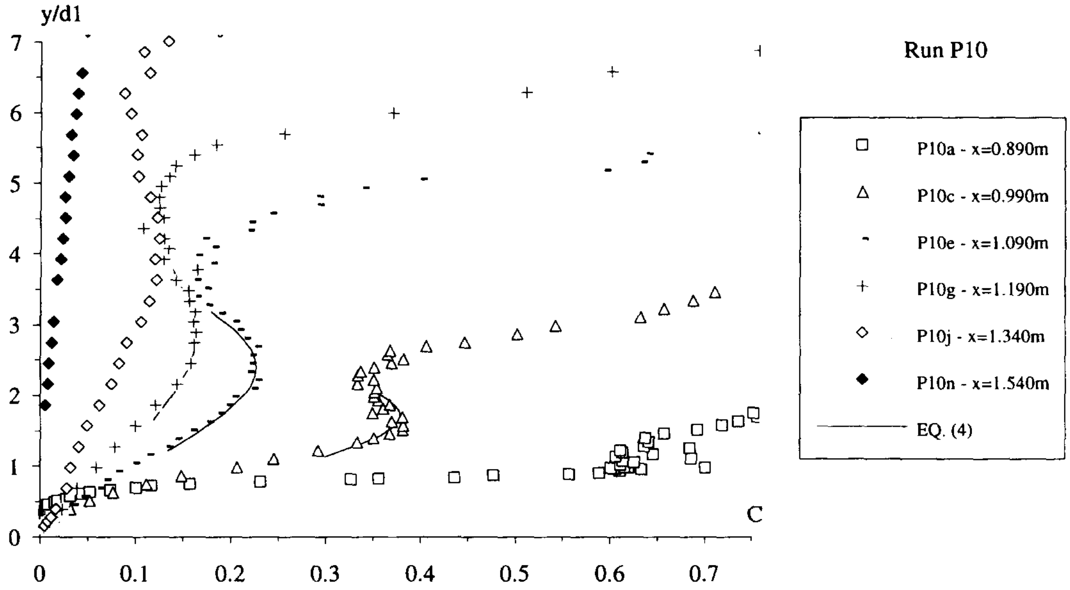

Fig. 2. Air concentration distributions—Run P10, $x_1 = 0.890$ m, $Fr_1 = 6.05$, $d_c = 0.0565$ m.

entrained. When the bubbles are diffused into regions of lower shear stresses, the coalescence of bubbles yields to larger bubble sizes and these bubbles are driven by buoyancy to the boiling region. Near the free-surface, the liquid is reduced to thin films separating the air bubbles. Their shape becomes pentagonal to decahedron as pictured by Thandaveswara (1974).

Characteristics of the turbulent shear region

Air concentration distributions were measured at the toe of the jump and along the jump. Typical profiles are plotted in Figs 2 and 3.

A major feature of the air concentration profiles is a region of high air content in the shear layer region immediately downstream of the intersection of the upstream flow with the roller (Figs 2 and 3). Other researchers observed a similar shape at hydraulic jumps with partially developed inflows: e.g. Resch and Leutheusser (1972), Resch *et al.* (1974) and Thandaveswara (1974), but fully developed hydraulic jumps and pre-entrained hydraulic jumps exhibit different air concentration distributions.

The analysis of several sets of experimental data (Table 3) shows that the air concentration distribution

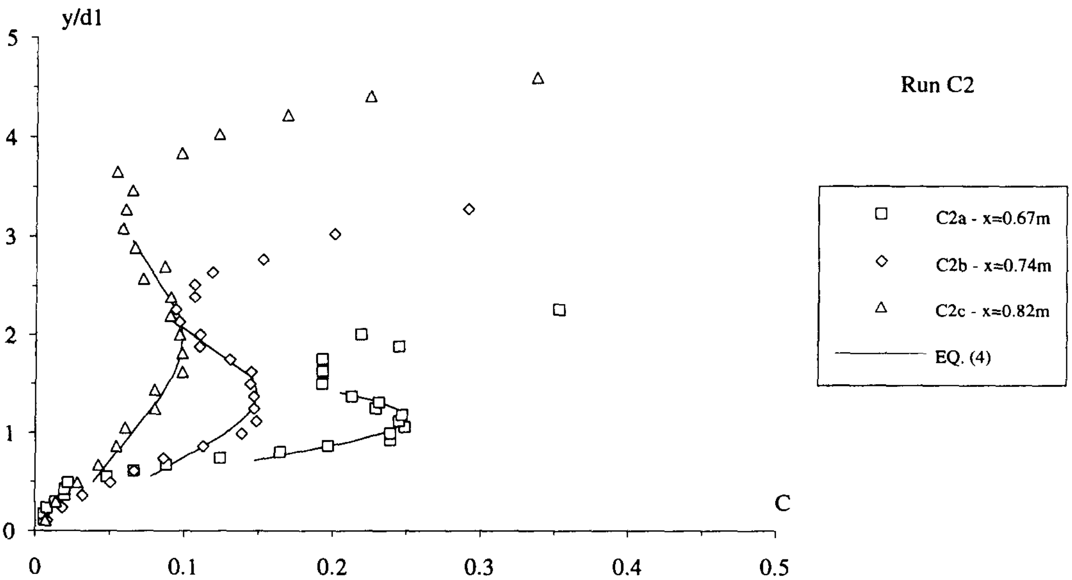

Fig. 3. Air concentration distributions—Run C2, $x_1 = 0.669$ m, $Fr_1 = 5.66$, $d_c = 0.0502$ m.

Table 3. Experimental flow conditions

Reference (1)	Run (2)	q_w (m²/s) (3)	Fr_1 (4)	x_1 (m) (5)	Comments (6)
Present study	C0	0.0504	8.11	0.963	$W = 0.25$ m
	C1	0.050	8.04	0.94	
	P10	0.0420	6.05	0.890	
	C2	0.0352	5.66	0.669	
	C3	0.0312	5.02	0.696	
Resch and Leutheusser (1972) and Resch *et al.* (1974)		0.0339	2.98*		Partially developed inflow.
		0.0718	8.04*		$W = 0.39$ m
Thandaveswara (1974)	R1	0.0302	7.16		"Normal hydraulic jump"
	R2	0.03484	7.41		with partially developed
	R3	0.04184	12.12		inflow. $W = 0.6096$ m
	R4	0.04887	12.52		
	R5	0.05612	13.31		
	R6	0.06086	10.33		

*Resch and Leutheusser (1972) indicated $Fr_1 = 2.85$ and 6.0. A re-analysis of their data suggests that $Fr_1 = 2.98$ and 8.04.

in the turbulent shear region follows a Gaussian distribution:

$$C = C_{max}*\exp\left(-\left(0.8063*\frac{y - y_{C_{max}}}{\Delta Y_{85\%}}\right)^2\right) \quad (4)$$

where C_{max} is the maximum air bubble concentration in the shear layer, $y_{C_{max}}$ is the location of the maximum air content. Equation (4) is plotted in Figs 2 and 3.

The experimental results indicate that C_{max} decays exponentially with the distance along the jump and it is best fitted by:

$$\frac{C_{max}}{(C_{max})_1} = \left(1 - \frac{x - x_1}{L_a}\right)^{1.993*Fr_1 - 6.083}$$

(data: present study) (5)

The other parameters of the air concentration distribution are correlated by:

$$(C_{max})_1 = 0.143*(V_1 - 0.21)$$

(present study, Resch and Leutheusser, 1972) (6)

$$\frac{y_{C_{max}} - d_1}{d_2 - d_1} = 1.101*\frac{x - x_1}{L_a}$$

(present study, Thandaveswara, 1978) (7)

$$\frac{\Delta Y_{85\%}}{d_1} = 0.07435*\frac{x - x_1}{d_1} + 0.324$$

(present study, Resch and Leutheusser, 1972) (8)

where $(C_{max})_1$ is the initial maximum air concentration, x is the distance along the channel and x_1 is the jump toe location. Note that equation (6) implies that there is no air entrainment for mean inflow velocities of less than 0.21 m/s. This result is consistent with previous observations (Table 1).

Air–water gas transfer

The turbulent shear region contributes substantially to the air–water gas transfer at a hydraulic jump: its large air content and the small bubble sizes resulting from large turbulent shear stress create a region of very large air–water interface area. The large air–water interface area enhances the gas transfer process.

With volatile gases, the air–water gas transfer is controlled by the liquid phase and the mass transfer across the air–water interface is usually estimated as:

$$\frac{d}{dt}C_{gas} = K_L*a*(C_s - C_{gas}) \quad (9)$$

where K_L is the mass transfer coefficient, a is the specific surface area, C_{gas} is the dissolved gas concentration and C_s is the saturation concentration. The driving force of the gas transfer process is the concentration gradient. When C_s is greater than C_{gas}, the gas will go into solution (i.e. dissolution). With $C_{gas} > C_s$ (i.e. supersaturation), the gas will desorb. Assuming quasi-spherical bubbles, an estimate of the air–water interface area is:

$$a = 6*\frac{C}{d_{ab}} \quad (10)$$

where C is a characteristic air concentration and d_{ab} is a representative air bubble size.

In the turbulent shear region (Fig. 1), the bubble sizes are controlled by the turbulent breakup process. Experimental data of maximum and mean bubble sizes in the turbulent shear region have been re-analysed. The results (Fig. 4) show that the maximum bubble size decreases with increasing upstream flow velocity. Indeed the upstream flow velocity is a measure of the level of turbulent shear stress in the shear layers of the jump and the maximum bubble diameter is expected to decrease with increasing shear stress. The maximum and mean bubble sizes in the shear flow region can be correlated by:

$$(d_{ab})_{max} = 0.230*V_1^{-3.93} \quad (1.5 < V_1 < 5 \text{ m/s}) \quad (11)$$

$$(d_{ab})_{mean} = 0.051*V_1^{-3.08} \quad (1.5 < V_1 < 5 \text{ m/s}) \quad (12)$$

Air–water gas transfer model

At a hydraulic jump, most air bubbles are entrained in regions of quasi-atmospheric pressure and the pressure variations are small. The temperature and salinity are usually constant. Hence most flow

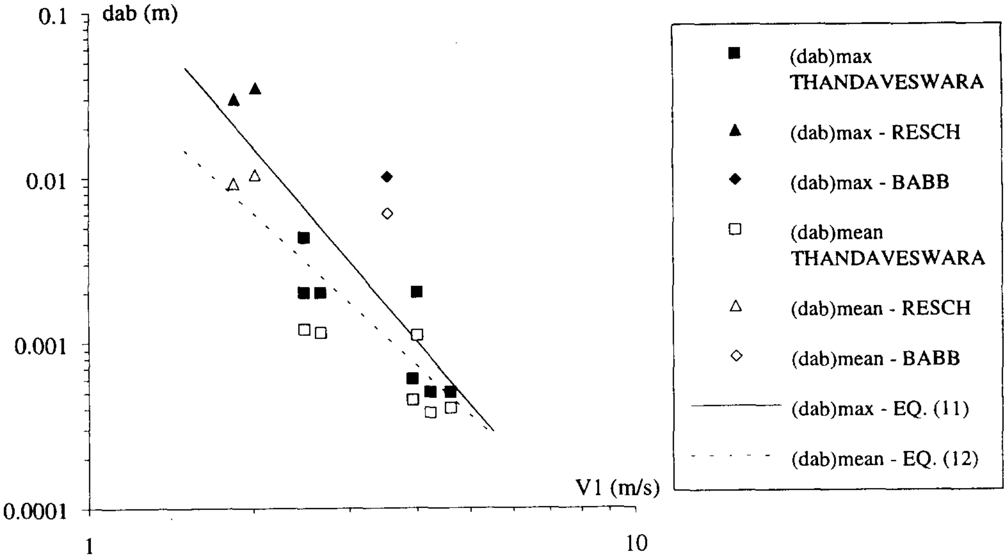

Fig. 4. Maximum and mean air bubble sizes in the shear flow region of hydraulic jumps (Thandaveswara, 1974; Resch *et al.*, 1974; Babb and Aus, 1981).

properties, including the coefficient of transfer (Kawase and Moo-Young, 1992) and the saturation concentration, become constants in equation (9).

Further, at a hydraulic jump with partially developed inflow, a major contribution to air–water gas transfer results from the small air bubbles entrained within the turbulent shear region (Figs 1, 2 and 3). In the shear region, the air–water interface area is of the order of magnitude of:

$$a \sim 6^* \frac{(C_{max})_1}{(d_{ab})_{max}} \qquad (13)$$

Integration of equation (9) then yields:

$$r \sim \exp(K_L{}^* a^* t) \qquad (14)$$

where t is the residence time of air bubbles and r is the deficit ratio. To a first approximation, the residence time can be approximated as:

$$t \sim 2^* \frac{L_a}{V_1} \qquad (15)$$

Equation (15) assumes that the air bubbles are entrained with a mean velocity equal to $V_1/2$ over the aeration region.

With these assumptions, an estimate of the air–water gas transfer at a hydraulic jump becomes:

$$r \sim \exp\left(12^* K_L{}^* \frac{(C_{max})_1}{(d_{ab})_{max}} * \frac{L_a}{V_1}\right) \qquad (16a)$$

where $(C_{max})_1$, $(d_{ab})_{max}$, L_a and V_1 are functions of the inflow conditions only and K_L is a function of the fluid properties. Replacing with equations (1), (6) and (11) yields:

$$r \sim \exp\left(13.057^* \frac{K_L}{\mathbf{g}} {}^* V_1^{4.93}{}^*(V_1 - 0.210)^* \frac{(\sqrt{1 + 8^* Fr_1^2} - 1)^*(Fr_1 - 1.5)}{Fr_1^2}\right) \qquad (16b)$$

Equations (14) and (16) enable estimatation of the gas transfer at a hydraulic jump with partially developed inflow.

DISCUSSION

Equation (16) has been compared with the data of Wilhelms *et al.* (1981). Wilhelms *et al.* injected concentrated solutions of krypton-85 upstream of a hydraulic jump and they recorded the downstream gas concentration. The saturation concentration for krypton-85 is zero and their experiments basically analysed the desorption of the gas. The mass transfer coefficient has been estimated using the correlation of Kawase and Moo-Young (1992) with a molecular diffusivity of krypton-85 in water of 1.92×10^{-9} m²/s at 25°C (Hayduk and Laudie, 1974).

The results are presented in Fig. 5 where the aeration efficiency*, computed with equation (16), is compared with the experimental data of Wilhelms *et al.* (1981). All the data were adjusted to 25°C using the correlation of APHA *et al.* (1989). Figure 5 shows a reasonable agreement between the data and computations. Some scatter is observed for the largest efficiencies and Froude numbers. At large Froude number, the air entrainment is important and visual

*More exactly the "de-aeration" efficiency.

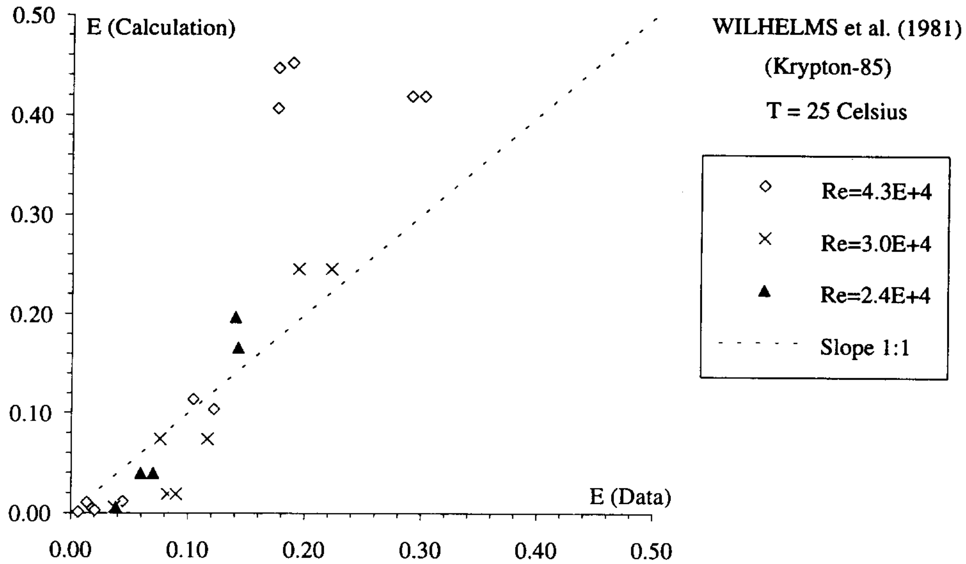

Fig. 5. Air–water transfer of krypton-85 at 25°C in terms of aeration efficiency—comparison between the data of Wilhelms *et al.* (1981) and the new gas transfer model [equation (16)].

observations indicate the existence of air pockets in which several air bubbles share the same interface. Bubble coalescence is also plausible. These mechanisms would induce a lower air–water interface [than predicted by equation (13)] and a smaller rate of aeration, but the differences between data and calculation might also result from measurements errors: Wilhelms *et al.* (1981) stated that "the reaeration rate coefficients vary greatly for replicate tests" and suggested additional tests at high Froude numbers.

Further, Fig. 6 shows a comparison of oxygen transfer calculations between the correlations of Avery and Novak (1978) and Wilhelms *et al.* (1981) and equation (16). The comparison is done within the range of the experimental studies (Table 2). The new model predicts an oxygen transfer of the same order of magnitude as experimental observations. Substantial differences are noted for large Froude numbers. These might be caused by a modification of the air-water flow structure (e.g. air pocket, coalescence) at large velocities but also by experimental errors: both

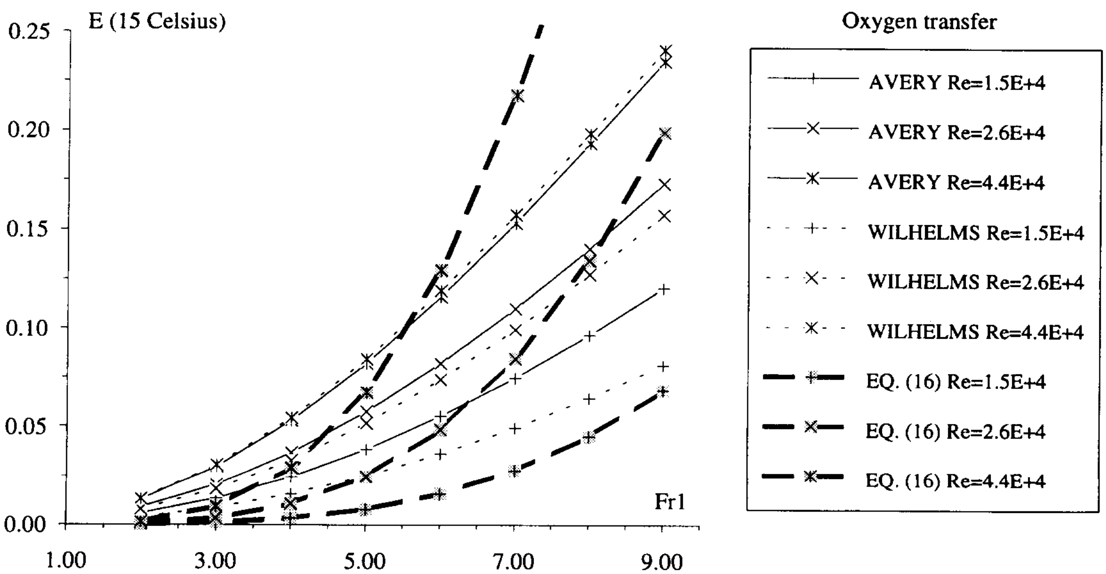

Fig. 6. Oxygen transfer at 15°C: aeration efficiency as a function of the upstream Froude number—comparison between the new gas transfer model [equation (16)] and the correlations of Avery and Novak (1978) and Wilhelms *et al.* (1981).

the data of Avery and Novak (1978) and Wilhelms *et al.* (1981) exhibited large errors for the largest Froude numbers.

CONCLUSION

In this study, the air bubble entrainment at hydraulic jumps with partially developed inflow has been investigated. The air–water flow is characterized by a turbulent shear region with a large air content. The turbulent shear region contributes substantially to the air–water gas transfer at the jump: its large air content and the small bubble sizes resulting from large turbulent shear stress create a region of large air–water interface area.

A new gas transfer model is developed based upon the air–water flow characteristics in the turbulent shear region. The new model shows a reasonable agreement with existing data. As the gas transfer model [equation (16)] is based upon physical evidence, it is believed that the new model will enable better gas transfer predictions on prototypes than existing empirical correlations. Further, equation (16) can be applied to any volatile gas and to both dissolution and desorption situations.

It must be noted that additional experiments are required for large Froude numbers and on prototypes to confirm the validity of the model.

Acknowledgements—This research project is supported by the Australian Research Council (Ref. No. A89331591). The author acknowledges the assistance of Dr B.S. Thandaveswara, Indian Institute of Technology, Madras and Ms G.L. Qiao, The University of Queensland, Australia.

REFERENCES

APHA, AWWA and WPCF (1989) *Standard Methods for the Examination of Water and Wastewater*, 7th edition. American Public Health Association, New York.

Apted R. W. and Novak P. (1973) Oxygen uptake at weirs. *Proc. 15th IAHR Congress*, Vol. 1, B23, Istanbul, Turkey, pp. 177–186.

Avery S. T. and Novak P. (1975) Oxygen uptake in hydraulic jumps and at overfalls. *Proc. 16th IAHR Congress*, C38, Sao Paulo, Brazil, pp. 329–337.

Avery S. T. and Novak P. (1978) Oxygen transfer at hydraulic structures. *J. Hydrol. Div., Am. Soc. civ. Engrs* **104,** 1521–1540.

Babb A. F. and Aus H. C. (1981) Measurements of air in flowing water. *J. Hydrol. Div., Am. Soc. civ. Engrs* **107,** 1615–1630.

Casteleyn J. A., Kolkman P. A. and Van Groen P. (1977) Air entrainment in siphons: results of tests in two scale models and an attempt at extrapolation. *Proc. 17th IAHR Congress*, Baden-Baden, Germany, pp. 499–506.

Chanson H. (1988) A study of air entrainment and aeration devices on a spillway model. Ph.D. thesis, Ref. 88-8, Department of Civil Engineering, University of Canterbury, New Zealand.

Chanson H. (1993) Characteristics of undular hydraulic jumps. Research Report No. CE146, Department of Civil Engineering, University of Queensland, Australia.

Chanson H. and Qiao G. L. (1994) Air bubble entrainment and gas transfer at hydraulic jumps. Research Report No. CE149, Deparment of Civil Engineering, University of Queensland, Australia.

Ervine D. A. and Ahmed A. A. (1982) A scaling relationship for a two-dimensional vertical dropshaft. *Proc. Int. Conf. on Hydraulic Modelling of Civil Engineering Structures*, BHRA Fluid Engineering, E1, Coventry, England, pp. 195–214.

Ervine D. A., Mckeogh E. and Elsawy E. M. (1980) Effect of turbulence intensity on the rate of air entrainment by plunging water jets. *Proc. Inst. civ. Engrs*, Part 2, pp. 425–445.

Hager W. H. (1992) *Energy Dissipators and Hydraulic Jump*, Vol. 8. Kluwer, Dordrecht, The Netherlands.

Hager W. H., Bremen R. and Kawagoshi N. (1990) Classical hydraulic jump: length of roller. *J. Hydrol. Res.* **28,** 591–608.

Hayduk W. and Laudie H. (1974) Prediction of diffusion coefficients for nonelectrolytes in dilute aqueous solutions. *AIChE Jl* **20,** 611–615.

Henderson F. M. (1966) *Open Channel Flow*. MacMillan, New York.

Holler A. G. (1971) The mechanism describing oxygen transfer from the atmosphere to discharge through hydraulic structures. *Proc. 14th IAHR Congress*, Vol. 1, A45, Paris, France, pp. 372–382.

Isaacs L. T. and Allen P. H. (1994) Contraction coefficients for radial sluice gates. *Proc. Int. Conf. on Hydraulics in Civil Engineering*, IEAust., Brisbane, Australia, 15–17 February, pp. 261–265.

Johnson P. L. (1984) Prediction of dissolved gas transfer in spillway and outlet works stilling basin flows. *Proc. 1st Int. Symp. on Gas Transfer at Water Surfaces* (Edited by Brutsaert W. and Jirka G. H.), pp. 605–612.

Kalinske A. A. and Robertson J. M. (1943) Closed conduit flow. *Trans. Am. Soc. civ. Engrs* **108,** 1435–1447.

Kawase Y. and Moo-Young M. (1992) Correlations for liquid-phase mass transfer coefficients in bubble column reactors with Newtonian and non-Newtonian fluids. *Can. J. Chem. Engng* **70,** 48–54.

Rabben S. L., Els H. and Rouve G. (1983) Investigation on flow aeration at offsets downstream of high-head control structures. *Proc. 20th IAHR Congress*, Moscow, USSR, Vol. 3, pp. 354–360.

Rajaratnam N. (1962) An experimental study of air entrainment characteristics of the hydraulic jump. *J. Inst. Engng India* **42,** 247–273.

Rajaratnam N. (1967) Hydraulic jumps. In *Advances Hydroscience* (Edited by Chow V. T.), Vol. 4, pp. 197–280. Academic Press, New York.

Resch F. J. and Leutheusser H. J. (1972) Le ressaut hydraulique: mesure de turbulence dans la région diphasique. *J. La Houille Blanche* **4,** 279–293.

Resch F. J., Leutheusser H. J. and Alemu S. (1974) Bubbly two-phase flow in hydraulic jump. *J. Hydrol. Div., Am. Soc. civ. Engrs* **100,** 137–149.

Thandaveswara B. S. (1974) Self aerated flow characteristics in developing zones and in hydraulic jumps. Ph.D. thesis, Department of Civil Engineering, Indian Institute of Science, Bangalore, India.

Wilhelms S. C., Clark L., Wallace J. R. and Smith D. R. (1981) Gas transfer in hydraulic jumps. Technical Report E-81-10, U.S. Army Engineer Waterways Experiment Station, CE, Vicksburg, MS.

Wisner P. (1965) Sur le rôle du critère de Froude dans l'etude de l'entraînement de l'air par les courants à grande vitesse. *Proc. 11th IAHR Congress*, Leningrad, USSR, Paper 1.15.